Laser and Particle Beams (1999), *vol.* 17, *no.* 1, *pp.* 109–117
Printed in the United States of America

Figure of merit for nonlinear materials in second-order cascaded nonstationary processes

By GUIDO TOCI, MATTEO VANNINI, AND RENZO SALIMBENI
Istituto di Elettronica Quantistica, Consiglio Nazionale delle Ricerche,
Via Panciatichi 56/30, 50127 Firenze, Italy

(Received 4 June 1998; Accepted 8 October 1998)

In this paper, we present and discuss an extension and an improvement of the Figure of Merit (FoM) that we introduced in a previous paper. The FoM describes the effectiveness of the frequency doubling materials for ultrashort light pulse modulators *via* second-order cascaded effects. In the present work, as an input pulse we use a temporal Gaussian pulse so that our perturbative method allows an analytical expression even for the output pulse field after the second pass inside the crystal. For the first time together with the completely analytical expression for the second pass, we report also the exact numerical coefficients for the peak phase modulation. With the FoM it is possible to choose the more appropriate nonlinear material and the use of the cascaded interaction process. Finally, we present for the first time the FoM dependence from the wavelength in the interval 0.5–1 μm, and to a table already shown we added more nonlinear materials.

1. Introduction

This paper presents a more complete study regarding what was previously mentioned on the so-called Figure of Merit (FoM) which results to be an important parameter for choosing nonlinear materials to be employed in second-order cascaded processes.

As it is well known in nonlinear optics, the input short pulse emitted by a passively mode-locked laser source can be functionally expressed by a hyperbolic secant or a Gaussian time dependence. Introducing a Gaussian pulse shape in our perturbative method reported elsewhere (Toci *et al.*, 1996a, 1996b, 1997, 1998), we were able to find for the first time analytical relations for the field even at the output of the second pass. The perturbative method describes the effects due to the self-phase and self-amplitude modulation of a light pulse with a type I second-order cascaded process in nonstationary conditions. This method accounts for the effects of the Group Velocity Mismatch (GVM) between the fundamental and the second harmonic pulse due to the material dispersion. Even in nonstationary conditions the phase modulation scales with the various parameters according to simple relations. Depending on the material and light pulse characteristic, there exists an optimal choice of the parameters for the excitation of the process.

In the optimized conditions, the phase modulation is proportional to a peculiar combination of the material parameters such as the nonlinear coefficient and the dispersion properties that we define as FoM. Because we employed a temporal Gaussian pulse as an input, we were able to find for the first time exact numerical coefficients for the phase modulation. To the table we previously presented (Toci *et al.* 1998), we added more nonlinear materials to obtain a more complete description of the available crystals for the second-order cascaded applications. Fur-

 0263-0346/99 $12.50

thermore, we plotted the wavelength dependence for the GVM, for the χ^2_{eff}, and finally according to equation (15) for the FoM.

2. Mathematical frame

The time-dependent equations for type I second harmonic generation (SHG) process with mismatched phase velocities are expressed by

$$\left(\frac{\partial}{\partial\xi}+\frac{1}{v_1}\frac{\partial}{\partial t}\right)\rho_1(\xi,t)=i\eta_0\,\rho_1(\xi,t)\rho_2(\xi,t)\exp(-i\delta\xi) \tag{1a}$$

for the fundamental (F) pulse and

$$\left(\frac{\partial}{\partial\xi}+\frac{1}{v_2}\frac{\partial}{\partial t}\right)\rho_2(\xi,t)=i\eta_0\,\rho_1^2(\xi,t)\exp(i\delta\xi) \tag{1b}$$

for the second harmonic (SH) pulse where $\omega_2=2\omega_1$ describes the SHG process, $v_{1,2}=\nu(\omega_{1,2})/L$ are the normalized group velocities (where L is the nonlinear crystal length), $\xi=z/L$ is the normalized longitudinal coordinate, $\delta=(k_2-2k_1)L$ is the phase mismatch parameter,

$$\rho_1(\xi)=\frac{E_1(\xi)}{|E_1(\xi=0)|_{pk}}\qquad\text{and}\qquad\rho_2(\xi)=\left[\frac{(k_2\cos^2\beta_2)}{(2k_1\cos^2\beta_1)}\right]^{1/2}\left[\frac{E_2(\xi)}{|E_1(\xi=0)|_{pk}}\right] \tag{2}$$

are the normalized field amplitudes, β_1 and β_2 are the birefringence angles for E_1 and E_2, and

$$\eta_0=\left[\frac{(4\pi\omega_1^2)}{(c^2\cos\beta_1\cos\beta_2)}\right]\left[\frac{2}{k_1k_2}\right]^{1/2}\chi^2_{eff}L|E_1(\xi=0)|_{pk} \tag{3}$$

is the normalized nonlinear coupling parameter in single-pass conversion efficiency and in stationary condition.

The analytical perturbative method previously reported (Toci *et al.* 1998) allows us to calculate the output F and SH pulses envelopes as a series development of the nonlinear coupling parameter η_0 for a given input F pulse shape, with the coefficients which are time dependent.

Using this approach, it appears that when the cascaded process is used to obtain a strong self-phase modulation of the incoming pulse (as required in the case of the so-called Cascaded Second-order Mode-locking, CSM, introduced by Cerullo *et al.* 1995a, 1995b) or to obtain an all-optical switching action, the so-called double-pass configurations are potentially more useful. In this kind of configuration, the fundamental pulse undergoes a first modulation process in the nonlinear crystal, where it also generates a second harmonic pulse. The two pulses are then reinjected into the crystal (or into another identical crystal) with the same propagation conditions, by means of an optical system which must allow a proper compensation of the phase and time delay between the two pulses. During the second pass the fundamental pulse undergoes a further self-modulation process, as well as a cross modulation induced by the residual second harmonic pulse. With a proper choice of the phase and the time delay, with this configuration it is possible to obtain a complete repumping of the F pulse, without energy losses toward a generated SH pulse. Nevertheless, for an incoming pulse duration with a duration comparable with or shorter than the crystal group delay $L[1/\nu_2-1/\nu_1]$ (that is, when the interaction occurs in nonstationary conditions), an unavoidable amplitude modulation process occurs, which perturbs the self-phase modulation process itself (Toci *et al.* 1998).

To define the Figure of Merit (FoM) for the materials involved in cascaded second order process in nonstationary conditions, we will deal with this class of configurations. In particular, we will consider the phase and amplitude modulation obtained with a $sech(t/\tau)$ or a Gaussian $[\exp(-t^2/\tau^2)]$ input F pulse shape. For this latter pulse shape, our method provides an

analytical expression for the pulse shape even at the output of the second pass and we report here all the calculations for the first time. Defining the auxiliary variables

$$u_1 = t/\tau, \tag{4}$$

$$\sigma = L[1/\nu_2 - 1/\nu_1]/2\tau, \tag{5}$$

$$y_1 = 8u_1\sigma - i\delta, \tag{6}$$

$$y_2 = 8u_1\sigma + 8\sigma\Delta t/\tau - i\delta, \tag{7}$$

where Δt is the time delay between the F and the SH pulse introduced by the optical system between the first and the second pass. At the lowest order of approximation in η_0 the fundamental field at the output of the second pass in a typical double-pass cascade is then given by

$$\rho_1 = e^{i\theta_1}\rho_{l,in}[1 + \eta_0^2(\exp[i(\delta + \theta_2 - 2\theta_1)]\gamma_2 + 2\gamma_1)], \tag{8}$$

where $\rho_{l,in}$ is the input pulse shape [either $\exp(-u_1^2)$ or $sech(u_1)$]; θ_1 and θ_2 are the overall phase delays accumulated by the F and the SH pulses, respectively, in the intrapass path; and γ_1 and γ_2 are auxiliary functions which in the case of a Gaussian input pulse have the form

$$\begin{aligned}\gamma_1 = {} & \frac{\sqrt{2\pi}}{8\sigma}\exp\left[\frac{-i\delta(16u_1\sigma - i\delta)}{32\sigma^2}\right] \\ & \times\left\{\frac{-(y_1 - 16\sigma^2)}{16\sigma^2}\left[\operatorname{erf}\left(\frac{\sqrt{2}}{8\sigma}(y_1 - 16\sigma^2)\right) - \operatorname{erf}\left(\frac{\sqrt{2}}{8\sigma}y_1\right)\right]\right. \\ & \left. + \cdots + \sqrt{\frac{2}{\pi}}\frac{1}{4\sigma}\left[\exp\left(-\frac{y_1^2}{32\sigma^2}\right) - \exp\left(-\frac{(y_1 - 16\sigma^2)^2}{32\sigma^2}\right)\right]\right\},\end{aligned} \tag{9}$$

$$\begin{aligned}\gamma_2 = {} & -\frac{\sqrt{2\pi}}{8\sigma}\exp\left[-\frac{i\delta}{32\sigma^2}\left(16\sigma\left(u_1 + \frac{\Delta t}{\tau} - 2\sigma\right) - i\delta\right)\right] \\ & \times\left\{\frac{1}{16\sigma^2}\left[(y_2 - 32\sigma^2)\operatorname{erf}\left(\frac{\sqrt{2}}{8\sigma}(y_2 - 32\sigma^2)\right) + y_2\operatorname{erf}\left(\frac{\sqrt{2}}{8\sigma}y_2\right)\right.\right. \\ & \left. - \cdots - 2(y_2 - 16\sigma^2)\operatorname{erf}\left(\frac{\sqrt{2}}{8\sigma}(y_2 - 16\sigma^2)\right)\right] \\ & \left. + \frac{\sqrt{2}}{4\sigma\sqrt{\pi}}\left[\exp\left(-\frac{(y_2 - 32\sigma^2)^2}{32\sigma^2}\right) + \exp\left(-\frac{y_2^2}{32\sigma^2}\right) - 2\exp\left(-\frac{(y_2 - 16\sigma^2)^2}{32\sigma^2}\right)\right]\right\},\end{aligned} \tag{10}$$

where $\operatorname{erf}(z) = [2/\sqrt{\pi}]\int_0^z \exp(-x^2)\,dx$ is the error function of complex argument z.

Conversely, in the case of a $sech(u_1)$ input pulse, the functions γ_1 and γ_2 assume the form of integral functions which unfortunately do not have closed analytical solution.

From equation (8), the nonlinear phase and amplitude modulation at the output of the first pass can be expressed as

$$\rho_1 = e^{i\theta_1}\rho_{l,in}\exp[(-\alpha_2 + i\phi_2)\eta_0^2], \tag{11}$$

where

$$\alpha_2 = -\operatorname{Re}[\exp[i(\theta_2 - 2\theta_1 + \delta)]\gamma_2 + 2\gamma_1], \tag{12}$$

$$\phi_2 = \operatorname{Im}[\exp[i(\theta_2 - 2\theta_1 + \delta)]\gamma_2 + 2\gamma_1], \tag{13}$$

are the nonlinear amplitude and phase modulation coefficient (a positive value of α_2 corresponds to an attenuation). At this order of approximation the phase and amplitude modulation are proportional to η_0^2.

We found that the best overall performance for the double–pass phase modulation process are obtained by setting the phase delay to $(\delta + \theta_2 - 2\theta_1) = 2n\pi$, and the time delay to $\Delta t = [1/\nu_2 - 1/\nu_1]L$. These conditions determine a complete repumping of the F pulse, without net energy losses toward a SH pulse, both for a Gaussian and for a *sech* incident pulse; furthermore they result in an intense nonlinear phase modulation profile, symmetric with respect to the pulse peak.

3. Scaling laws for the process parameters

Looking at the phase and amplitude modulation profiles obtained with a $sech(t/\tau)$ or a Gaussian input pulse shape, we can underline the following behaviors, which are common to both pulse shapes:

- For a given crystal length, when the pulse duration decreases and the steadiness parameter σ [see equation (5)] increases, the phase modulation coefficient ϕ_2 exhibits a broad and flat maximum with respect to σ (about $\sigma = 1.4$ in the specified conditions) at the center of the pulse and then decreases monotonically, (see figure 1a).
- After such a maximum, the phase modulation profile broadens temporally and develops several satellite peaks.

Similarly at the same point, the amplitude modulation shows a fast growth (see figure 1b), and the value of σ which determines the occurrence of the maximum in the phase modulation profile can be considered as the threshold for the onset of a real nonstationary interaction.

Looking at the phase modulation coefficient at the center of the pulse, we can also notice the following properties:

- the peak value of the phase modulation is inversely proportional to δ (approximately $\phi_{pk} \approx 0.7\pi/|\delta|$ both for *sech* and Gaussian unchirped pulses); figure 2a.
- the threshold value for σ which determines the onset of the nonlinear interaction is proportional to δ ($\sigma_{pk}(\delta) \approx 0.5|\delta|/\pi$ for *sech* pulses, $\sigma_{pk}(\delta) \approx 0.35|\delta|/\pi$ for Gaussian pulses); figure 2b.

It follows that for a given pulse duration τ and crystal length L (that is a given value of σ), there exists an optimum value of the phase mismatch parameter δ for which $\sigma = \sigma_{pk}$ (corresponding to $|k_2 - 2k_1| = \pi(1/\nu_2 - 1/\nu_1)/\tau$ for a *sech* pulse) and which determines a coherence length about equal to the longitudinal walkoff length.

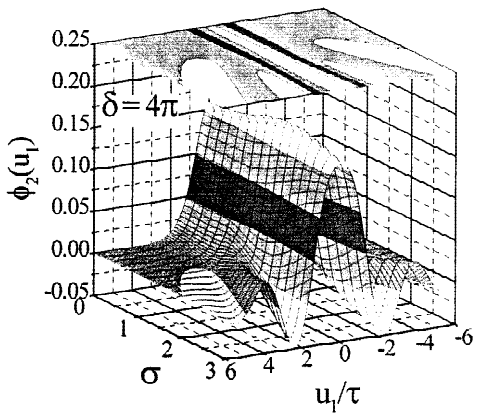

FIGURE 1A. Second-order nonlinear phase modulation coefficient ϕ_2 for a *sech* pulse, at the output of the second pass, with optimized phase and temporal delay, for $\delta = 4\pi$.

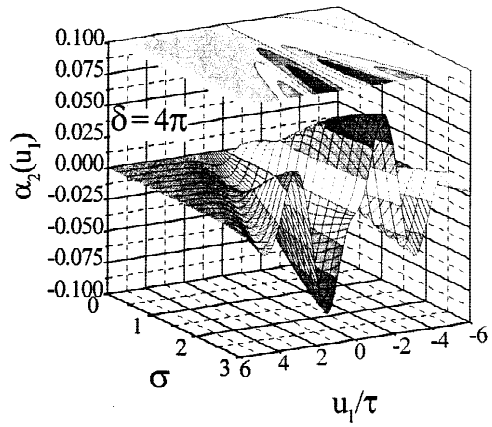

FIGURE 1B. Second-order nonlinear amplitude modulation coefficient ϕ_2 for a *sech* pulse, at the output of the second pass, with optimized phase and temporal delay, for $\delta = 4\pi$.

4. Figure of Merit (FoM) for cascaded processes

In the above-described conditions, the expression for the peak phase modulation is given by

$$\phi_{pk} = 0.7\left(\frac{4\omega_1^2}{c^2\cos^2\beta_1\cos^2\beta_2}\right)\left[\frac{(\chi^2_{eff})^2}{n_1 n_2(1/\nu_2 - 1/\nu_1)}\right]|E_1|^2_{pk}\tau L. \tag{14}$$

The term in square brackets depends only on the material properties, and it is independent from the pulse parameters and the other excitation conditions. We can therefore define the FoM for a nonlinear material employed for transient second-order cascaded effects as

$$M = \left[\frac{(\chi^2_{eff})^2}{n_1 n_2(1/\nu_2 - 1/\nu_1)}\right], \tag{15}$$

which accounts both for the material nonlinear properties and its dispersion characteristics, and summarizes their effects on the self-phase modulation process.

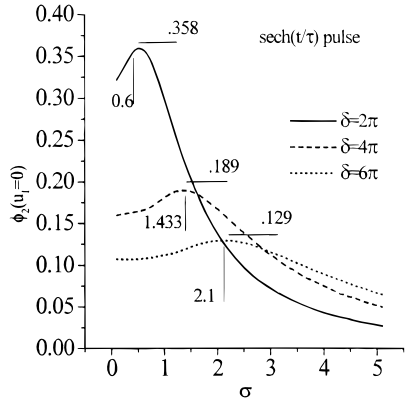

FIGURE 2A. Second-order nonlinear amplitude modulation coefficient ϕ_2 for a *sech* pulse, evaluated at the pulse center ($u_1 = 0$) as a function of the steadiness parameter σ, for various values of the phase mismatch δ.

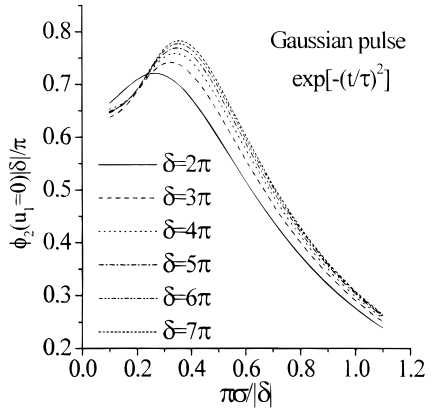

FIGURE 2B. Second-order nonlinear amplitude modulation coefficient ϕ_2 for a Gaussian pulse, normalized to δ, evaluated at the pulse center ($u_1 = 0$) as a function of the steadiness parameter σ (rescaled with δ), for various values of the phase mismatch δ.

The FoM shows a quite large variation among the most widely used nonlinear materials, and a strong dependence from the wavelength.

The evaluation of this FoM provides a guideline for the choice of the nonlinear material for specific devices or experiments based on the second-order cascaded processes.

We have calculated the FoM, *M*, for the type I, second-order cascaded interaction at $\lambda =$ 1064 nm for several commonly employed nonlinear materials; for each material the value of the various parameters was calculated using the suitable phase-matching angles and polarization directions.

The choice of the materials described in Table 1 was determined mainly by the fact that they are used as frequency doubling materials (KDP and isomorphs, BBO, $LiIO_3$, MgO:$LiNbO_3$) and in some cases they were already employed for the excitation of second-order cascaded effects in nonstationary conditions (LBO). Other materials, although less used or only recently proposed, could be interesting, such as urea, an organic compound with a rather large second-order nonlinearity, or the $K_2La(NO_3)_5$:$2H_2O$ (KLN), a material belonging to the nitrate compound class. The latter allows noncritical phase matching close to room temperature in the near infrared (Ebbers *et al.* 1993).

Table 1 summarizes the main results. We can see that *M* undergoes a quite large variation over the considered materials, and an estimation of the overall performance based on a reduced subset of parameter can even be misleading. For instance, we can see that the KDP and its isomorphs (ADP, KD*P, RDP) exhibit a rather low GVM, making them attractive, at a first glance, for the excitation of transient cascaded processes; but a comparative analysis based on the evaluation of *M* evidences that their rather low value of χ^2_{eff} determines an overall performance which is the lowest among the considered materials. This is particularly true for the RDP, as it even lacks the advantage of a low GVM. The situation is reversed for the $LiIO_3$ and for the urea, which have an interesting strong nonlinear coefficient. On the other hand, the value of the GVM is so high that the overall performance of the material is almost impaired, mainly in the case of the urea. The BBO provides the better performance among the considered materials despite its quite high GVM, due to its large nonlinear coefficient which allows the use of short samples.

The MgO:$LiNbO_3$ was included as a representative of the niobate compound class, because it exhibits interesting nonlinear and phase-matching properties. Both its nonlinear coefficient and its GVM are very large, several times those shown by the BBO for instance, and they

TABLE 1. Figure of Merit M and propagation parameters for several commonly used nonlinear materials.

Material	n_1, n_2	χ^2_{eff} $[(\mathrm{cm}^3/\mathrm{erg})^{1/2}]$	GVM $(1/v_2 - 1/v_1)$ (ps/cm)	M $(\mathrm{cm}^4/(\mathrm{erg\ s}))$	Phase-matching scheme	Reference
BBO	1.6420	4.27×10^{-9}	0.8500	7.97×10^{-6}	Angle	Kato 1986 Eckardt *et al.* 1990
$MgO:LiNbO_3$	2.224	-1.12×10^{-08}	5.59	4.55×10^{-6}	Temp.	Nightingale *et al.* 1986 Eckardt *et al.* 1990
$MgO:LiNbO_3$	2.224	-1.11×10^{-08}	5.69	4.37×10^{-6}	Angle	Nightingale *et al.* 1986 Eckardt *et al.* 1990
LBO	1.5900	1.98×10^{-9}	.5500	2.82×10^{-6}	Temp.	Velsko *et al.* 1991
KLM	1.548	-2.75×10^{-9}	1.31	2.41×10^{-6}	Temp.	Ebbers *et al.*1993
$LiIO_3$	1.8570	4.89×10^{-9}	2.890	2.40×10^{-6}	Angle	Eckardt *et al.* 1990 Weber 1986
ADP	1.5070	8.42×10^{-10}	0.1341	2.33×10^{-6}	Angle	Ghosh & Bhar 1982 Sutherland 1996
KDP	1.4940	5.98×10^{-10}	0.0870	1.84×10^{-6}	Angle	Ghosh & Bhar 1982 Sutherland 1996
KD*P	1.4690	5.51×10^{-10}	0.0935	1.50×10^{-6}	Angle	Ghosh & Bhar 1982 Sutherland 1996
Urea	1.5472	2.38×10^{-9}	2.00	1.18×10^{-6}	Angle	Halbout *et al.* 1979
RDP	1.491	7.58×10^{-10}	0.865	2.99×10^{-7}	Angle	Weber 1986 Sutherland 1996

compensate each other yielding the highest performance, apart from the BBO. The MgO: $LiNbO_3$ was included twice because at 1064 nm it allows both angle phase matching at room temperature, and noncritical phase matching at 108°C for 5% MgO concentration (Nightingale *et al.* 1986).

The KLN exhibit an overall performance similar to the $LiIO_3$, but with the advantage that it exhibits noncritical phase matching at room temperature.

We have also investigated the wavelength dependence of the FoM and of the parameters which concur to its evaluation, for three commonly employed nonlinear materials.

In the evaluation of χ^2_{eff} as a function of wavelength, we have neglected the wavelength dispersion of the elements of the second-order nonlinear optical tensor which usually exhibit a rather weak wavelength dependence (actually seldom reported in literature). The main contribution to the wavelength dependence of χ^2_{eff} results from the phase-matching conditions, which determines the directions of the field polarizations with respect to the optical axes. Figure 3 reports the GVM, and figure 4 reports χ^2_{eff} as a function of wavelength. The FoM for the three materials obtained by plotting equation (15) is reported in figure 5. We can see that for some materials M exhibits a rather strong wavelength dependence, and in particular for short wavelengths the performance of the $LiIO_3$ appears more interesting than the BBO, despite occurring at 1064 nm.

5. Conclusions

We reported here a definition of a Figure of Merit (FoM) for the frequency doubling nonlinear materials to be employed in the second-order cascaded processes excited by ultrashort pulses.

This FoM allows us to evaluate the effectiveness of the nonlinear materials and it is useful to compare their relative performances in a given experimental situation.

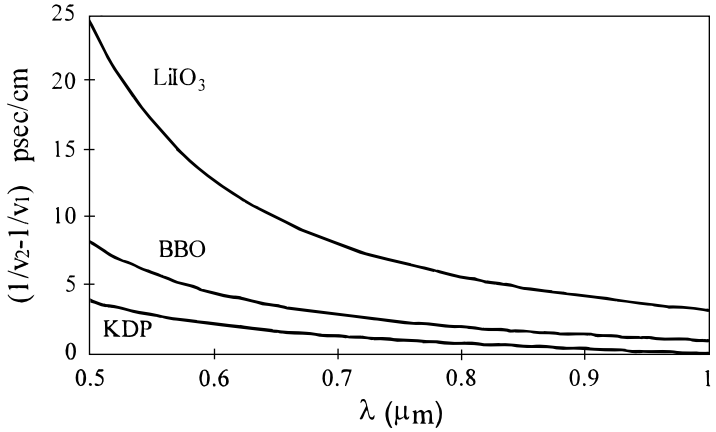

FIGURE 3. Wavelength dependence of the GVM for BBO, $LiIO_3$, and KDP in conditions of matched phase velocities.

The proposed FoM results from the balance of the nonlinear and of the dispersion properties of the material. For instance, a material with a rather high nonlinear coefficient such as the $LiIO_3$ exhibits a rather poor performance due to the very high GVM, with respect to the LBO and BBO which are a better compromise between nonlinear and dispersion properties.

The FoM has also a significant wavelength dispersion, which is due not only to the GVM wavelength dependence, but also to the fact that the effective nonlinear coefficient χ^2_{eff} depends on the phase-matching angle, and this last has a strong dependence on the wavelength.

Our results show that a good choice of the proper nonlinear materials for the design of experiments or devices using the cascaded process at a given wavelength is helped by the use of the above discussed FoM. Nevertheless, there are other material parameters which become important when dealing with finite aperture or focused beams, such as the angular acceptance and the lateral beam walkoff due to the material birefringence. In this sense, the BBO and even more the $LiIO_3$ have both a rather low angular acceptance and a rather high walkoff, whereas the large acceptance angle and the null walkoff achievable with temperature phase matching in

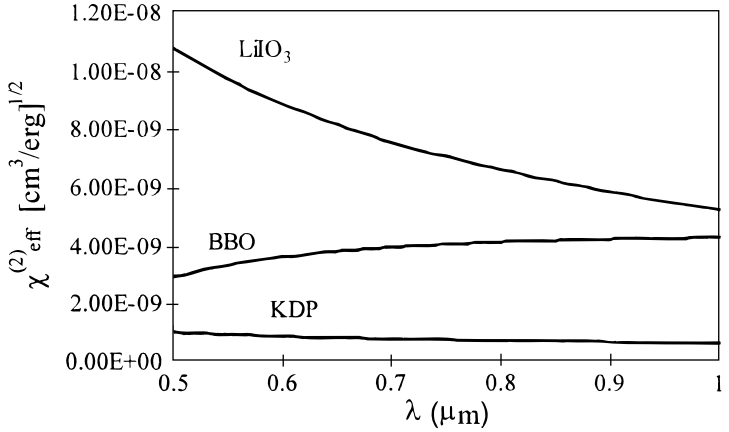

FIGURE 4. Wavelength dependence of the nonlinear second-order coefficient for BBO, $LiIO_3$, and KDP in conditions of matched phase velocities.

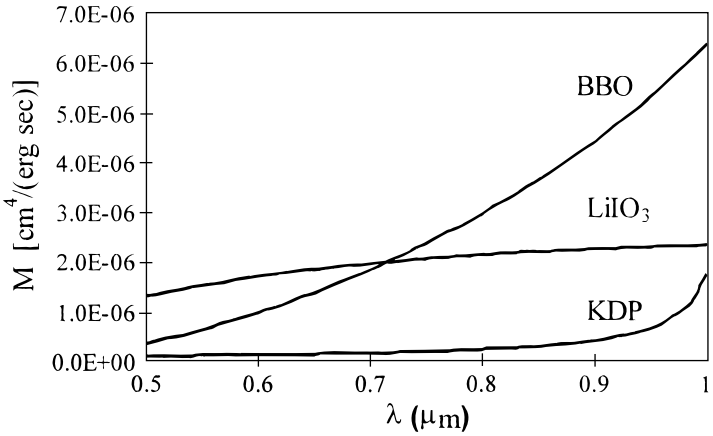

FIGURE 5. Wavelength dependence of the figure of merit M for the cascaded second-order nonlinear process for BBO, $LiIO_3$, and KDP.

LBO and conceivably with the KLM, as well as their reasonably high value of M make them attractive materials. Indeed, the LBO was successfully employed for the passive laser-mode locking through the second-order nonlinearity (Danailov *et al.* 1994; Cerullo *et al.* 1995a, 1995b). The peak-phase modulation, equation (14), can be completely obtained analytically if we use as input pulse a temporal Gaussian one. To better characterize the nonlinear materials, we studied and we report here the dependence of the FoM from the wavelength. According to a chosen interval, a material such as the BBO can become more efficient as in the mid-infrared where its FoM is higher than that of the widely used LBO. More materials are finally added to table 1 making it more useful for people working with second-order nonlinear effects.

REFERENCES

CERULLO, G. *et al.* 1995a *Opt. Lett.* **20**, 746.

CERULLO, G. *et al.*1995b *Opt. Lett.* **20**, 1785.

DANAILOV, M.B. *et al.* 1994 *Opt. Lett.* **19**, 792.

EBBERS, C.A. *et al.* 1993 *IEEE J. Quant. Electron.* **QE-29**, 497.

ECKARDT, R.C. *et al.* 1990 *IEEE J. Quant. Electron.* **QE-26**, 922.

GHOSH, G.C. & BHAR G.C. 1982 *IEEE J. Quant. Electron.* **QE-18**, 143.

HALBOUT, J.M. *et al.* 1979 *IEEE J. Quant. Electron.* **QE-15**, 1176.

KATO K. 1986 *IEEE J. Quant. Electron.* **QE-22**, 1013.

NIGHTINGALE, J.L. *et al.* 1986 *Proc. SPIE* **681**, 20.

SUTHERLAND, R.L. 1996 *Handbook of Nonlinear Optics* (M. Dekker, New York).

TOCI, G. *et al.* 1996a *Proceedings of the International Conference on Laser '95,* Vol. 761 (STS Press, McLean, Virginia).

TOCI, G. *et al.* 1996b *Ultrafast Processes in Spectroscopy,* Vol. 179 (Plenum Press, London, New York).

TOCI, G. *et al.* 1997 *Opt. Commun.* **143**, 156.

TOCI, G. *et al.* 1998 *J. Opt. Soc. Am. B* **15**, 103.

VELSKO, S.P. *et al. 1991 IEEE J. Quant. Electron.* **QE-27**, 2182.

WEBER, M.J. 1986 *CRC Handbook of Laser Science and Technology,* Vol. III (CRC Press Inc., Boca Raton, Florida).